FDA approved calcium channel blockers inhibit SARS CoV 2 infectivity in epithelial lung cells

Marco R. Straus[1], Miya Bidon[2], Tiffany Tang[2], Gary R. Whittaker[1*] and Susan Daniel[2*]

[1]Department of Microbiology and Immunology, Cornell University, Ithaca, NY, 14853, USA

[2]Robert Frederick Smith School of Chemical and Biomolecular Engineering, Cornell University, Ithaca, NY, 14853, USA

*Corresponding authors:

Gary Whittaker: grw7@cornell.edu

Susan Daniel: sd386@cornell.edu

Abstract

Covid-19 has infected more than 14 million people worldwide causing over 600.000 deaths[1]. The disease is caused by the severe acute respiratory syndrome coronavirus (CoV) 2 (SARS-CoV-2), which shares a high sequence similarity to SARS CoV[2]. Currently there are no vaccinations available to provide protection and the only antiviral therapy in active use in patients is remdesivir, which currently provides only limited benefit[3]. Hence, there is an urgent need for antiviral therapies against SARS CoV 2. SARS CoV requires Ca^{2+} ions for host cell entry[4] and based on the similarity between SARS CoV and SARS CoV 2[5] it is highly likely that the same requirements exist for the two viruses. Here, we tested whether FDA-approved calcium channel blocker (CCB) drugs are efficacious to inhibit the spread of SARS CoV 2 in cell culture. Our data shows that amlodipine, felodipine and nifedipine limit the growth of SARS CoV 2 in epithelial kidney (Vero E6) and epithelial lung (Calu-3) cells. We observed some differences in the inhibition efficacy of the drugs in the two different cell lines, but with felodopine and nifedipine having the greatest effect. Overall, our

data suggest that CCBs have a high potential to treat SARS CoV 2 infections and their current FDA approval would allow for a fast repurposing of these drugs.

Introduction

Coronaviruses (CoVs) are major zoonotic pathogens that cause respiratory and/or enteric tract infections in a variety of species including humans. Most CoVs that are pathogenic to humans cause only mild cold-like disease symptoms[6]. However, in 2002 the highly pathogenic severe acute respiratory syndrome (SARS) CoV emerged followed by the middle east respiratory syndrome (MERS) CoV in 2012. SARS-CoV and MERS-CoV exhibited case fatalities rates of 11% and 34%, respectively, and patients infected with either SARS CoV or MERS CoV expressed very similar clinical symptoms[7–10]. Currently, the worldwide Covid-19 outbreak caused by the Severe Acute Respiratory Syndrome (SARS) CoV 2 poses a dramatic risk to public health worldwide[11]. The virus was first identified in December 2019 in Wuhan, China and since has spread all over the globe[12]. To this date, there are no vaccines or highly efficacious drugs available against SARS CoV, MERS CoV, or SARS CoV 2.

In the US, the Food and Drug Administration (FDA) authorized three drugs for use against Covid-19 which are the RNA dependent RNA polymerase inhibitor remdesivir, initially developed for Ebola treatment, and the two anti-malaria drugs chloroquine and hydroxychloroquine. However, while the latter two have been proven to not be suitable for Covid-19 treatment, remdesivir was shown some improvement in symptoms of 68% of treated patients in clinical trials[3,13]. Overall, there remains need to identify and to provide additional drugs that help to treat Covid-19 patients. Given the current pandemic and the need for expediency, ideally, these drugs are already FDA approved and therefore need to be only repurposed, avoiding the lengthy approval process.

Current antiviral therapies often target virus replication or virus release; examples being remdesivir or influenza neuraminidase inhibitors, respectively[3,14]. A viable target for a potential drug is the viral entry of the virus into the host cells as this is a crucial step in the viral life cycle[5]. For SARS-CoV, SARS-CoV 2 and MERS-CoV the spike (S) protein mediates binding to the respective receptor via its S1 domain and initiates the fusion with the host cell via its S2 domain[5]. For SARS-CoV and MERS-CoV, the S protein has been studied extensively and it becomes more and more apparent that SARS-CoV-2 S functions in a very similar fashion[5]. Previous studies have revealed that SARS-CoV and MERS-CoV utilize calcium ions (Ca^{2+}) that are coordinated by amino acid residues within the fusion peptide to form a fusion loop that integrates into

the host cell membrane[4,15]. Depleting intracellular and/or extracellular Ca^{2+} resulted in full suppression of viral entry for SARS CoV and partial reduction of viral fusion of MERS CoV. Sequence comparisons have shown that the fusion domains of SARS CoV and SARS CoV 2 are virtually identical and hence, strongly suggesting that the same Ca^{2+}-dependency for viral entry exists for SAR- CoV-2[5].

The crucial role of Ca^{2+} in the viral entry of CoVs prompted us to explore whether FDA approved Ca^{2+} channel blocker (CCB) drugs have the potential to inhibit viral growth of SARS-CoV-2. We chose five drugs from different classes that all inhibit high voltage-activated Ca^{2+} channels of the L-type. We selected the dihydropyridines: amlodipine, nifedipine and felodipine; the phenylalkylamine: verapamil; and the benzothiazepine: diltiazem. These five drugs are primarily used to treat cardio-vascular diseases. In addition, we also tested the FDA-approved Ca^{2+} chelator drug: diethylenetriaminepentaacetic acid (DTPA), which is used against radioactive contaminations of internal organs.

Results

Amlodipine, nifedipine, felodipine and verapamil inhibit SARS-CoV-2 infection of Vero E6 cells

To test the whether the five CCBs and the Ca^{2+} chelator DTPA inhibit growth of SARS-CoV-2, we infected Vero E6 cells at a MOI of 0.1 and added four different concentrations of each compound immediately post infection. The tested concentrations were 10 µM, 50 µM, 100 µM and 500 µM and viral titers were analyzed 24 hours post infection. For amlodipine, we observed a 5-log reduction of viral growth at 50 µM and we were not able to detect any viral titer at a concentration of 100 µM (Figure 1A). However, amlodipine also exhibited a 25% reduction of cell viability at a concentration of 50 µM, which increased to 90% at 100 µM and 500 µM (Figure 2A). Nifedipine only reduced viral titers by 5 logs at a high concentration (500 µM) and expressed about 15% cytotoxicity (Figure 1A and 2A). Felodipine completely suppressed growth of SARS CoV 2 at a concentration of 50 µM with no statistically significant cytotoxicity (Figure 1A and 2A). 100 µM verapamil reduced the viral titers by 50% compared to the untreated control without a cytotoxic effect (Figure 1A and 2A). Diltiazem reduced viral growth at 500 µM but also compromised cell viability at this concentration and DTPA showed no effect (Figure 1A and 2A).

Nifedipine and felodipine suppress SARS-CoV-2 infection of epithelial lung cells

Vero E6 cells are a good model system for SARS-CoV-2 infections, but the cell line is derived from epithelial kidney cells and may not represent the virus-drug-cell interactions in the lung. Therefore, we tested the CCBs and the Ca^{2+} chelator DTPA in the epithelial lung cell line Calu-3. The results for amlodipine were comparable to what we found in Vero cells (Figure 1B and 2B). Nifedipine and felodipine, however,

significantly inhibited viral growth at lower concentrations compared to what was observed in Vero E6 cells. Nifedipine reduced the viral titers by 1.5 logs at a concentration of 100 µM and no virus was detectable at 500 µM while cytotoxicity was moderate (Figure 1B and 2B). Felodipine diminished SARS-CoV-2 growth by half at 10 µM and at 50 µM no virus was detected anymore with no cytotoxic effect (Figure 1B and 2B). In contrast, verapamil had a weakened inhibitory effect at 100 µM compared to Vero E6 cells (Figure 1B and 2B). As in Vero cells, 100 µM verapamil fully suppressed viral growth but also compromised cell viability by about 90%. We found very modest infection inhibition for diltiazem and DTPA at non-cytotoxic concentrations of 500 µM and 100 µM, respectively (Figure 1B and 2B).

Discussion

Overall, of the tested CCBs, felodipine provides the best candidate drug for repurposing. Felodipine fully inhibited growth of SARS-CoV-2 in both tested cell types at a concentration of 50 µM while we did not observe significant cytotoxicity (Figure 1 and 2). Nifedipine is another promising candidate as it suppressed viral growth particularly well in epithelial lung cells at concentrations that were not cytotoxic (Figure 1 and 2). Application of all other tested CCBs resulted in reduced titers too, but their effect seemed to be inferior compared to felodipine and nifedipine. Amlodipine treatment resulted in very low or undetectable titers but even low concentrations of the drug had cytotoxic effects. Verapamil and diltiazem application led to partially reduced SARS CoV 2 growth in Vero cells, but suppressed growth only to a minor extent in Calu-3 cells (Figure 1 and 2). The Ca^{2+} chelator DTPA had no major effect in the tested cell lines. In conclusion, felodipine and nifedipine represent strong drug candidates for the treatment of Covid-19.

The observed inhibition differences in the different cell lines suggest that inhibition may occur at the level of host cell entry. In Vero cells, CoVs preferentially enter the host cells via the endocytic pathway utilizing endosomal proteases, such as cathepsins, for S protein activation[5,16]. Calu-3 cells, on the contrary, are predominantly infected via plasma membrane fusion and cleavage of S is mediated by TMPRSS2 and furin[5,17]. Felodipine and nifedipine was more efficacious in Calu-3 cells at concentrations of 10 µM and 50 µM compared to Vero cells, respectively. In contrast, 100 µM verapamil reduced viral growth in Vero cells by 3 logs but there was barely a reduction of viral titers in Calu-3 cells. Others that have previously reported that CCBs inhibit viral infections at the cell entry level. Influenza A infections, for example, trigger an influx of Ca^{2+} which assists the endocytic uptake of the virus while treatment with verapamil or diltiazem inhibits viral infection[18–20]. New World hemorrhagic fever arenaviruses, such as the Junin virus, are reportedly sensitive to CCBs and treatment with CCBs blocks the entry of the virus into the host cell[21].

However, the exact mechanism how CCBs suppress SARS-CoV-2 infection needs to be addressed in a separate study. CCBs were also shown to interfere with viral infections of several other viruses (e.g. Japanese Encephalitis virus, Zika virus, Dengue virus) at the stage of viral replication[22], thus until further study, it cannot be excluded that CCBs can inhibit SARS-CoV-2 propagation at different stages, including virus release.

Covid-19 infections typically manifest in the upper respiratory tract[23]. Therefore, it is important to emphasize that felodipine and nifedipine work with higher efficiency in the lung cell line Calu-3 compared to the kidney epithelial Vero E6 cells (Figure 1A and 1B). In this context, it is noteworthy that CCBs are believed to not only affect cardiovascular muscles but also airway smooth muscle cells, which rely on L-type calcium channels for their contraction[24–26]. A recent study using the CCBs tested here for their potential to improve lung function in asthma patients and concluded there was a beneficial effect, providing evidence that CCBs act in the lungs[27]. This also links to the observation that asthma is not on the top ten list of chronic health problems that people suffered from who died of Covid-19 as one would expect this respiratory condition to be. Nebulizers used for asthma medications are supplemented with EDTA as a preservative which may help to deplete extracellular Ca^{2+}[27] supporting the idea that interfering with cellular Ca^{2+} affects SARS CoV 2 growth.

CBBs have a high potential to treat Covid-19 patients

In summary, we provide strong evidence that CBBs, in particular nifedipine and felodipine, inhibit infection of SARS-CoV-2 in lung cells and hence, present a high potential to treat Covid-19 patients. There is already evidence that nifedipine and amlodipine decrease mortality and the risk for intubation and ventilation in elderly Covid-19 patients[28]. Therefore, we believe that CCBs, possibly in combination with remdesivir, could provide the relief for Covid-19 patients until vaccines have been successfully developed**.** Moreover, CCBs could represent a novel class of antiviral therapeutics against a variety of viruses including MERS-CoV and SARS-CoV and those yet to emerge, given the strong conservation of the Ca^{2+} binding region in CoVs.

Figure legends

Figure 1: Inhibitory effect of five CCBs and the Ca^{2+} chelator DTPA on SARS-CoV-2 infection. (A) Vero E6 epithelial kidney cells were infected with SARS-CoV-2 isolate USA-WA1/2020 at an MOI of 0.1 for 24 hours. (B) Calu-3 epithelial lung cells were infected with SARS-CoV-2 isolate USA-WA1/2020 at an MOI of 0.1 for

24 hours. The CBBs amlodipine, nifedipine, felodipine, verapamil and diltiazem and the chelator DTPA were added to the cells at the indicated concentrations immediately after the virus. TCID50s were performed with growth supernatants and calculated according to the Reed-Muench method[30]. No bar means no virus was detected at the respective concentration. Error bars represent standard deviations (n = 3). Asterisks indicate statistical significance compared to the untreated control. Statistical analysis was performed using an unpaired Student's t-test. * = P > 0.05, ** = P > 0.01, *** = P > 0.001.

Figure 2: Cytotoxic effect of the five CCBs and the Ca^{2+} chelator DTPA on cells. (A) Vero E6 epithelial kidney cells and (B) Calu-3 epithelial lung cells were treated with the indicated concentrations of amlodipine, nifedipine, felodipine, verapamil, diltiazem and DTPA for 24 hours. After 24 hours cell viability was measured using 3-(4,5-dimethylthiazol-2-yl)-2,5-diphenyltetrazolium bromide (MTT). Cell viability was determined by normalizing absorbance from the sample well by the average absorbance of untreated wells. Error bars represent standard deviations (n = 3). Asterisks indicate statistical significance compared to the untreated control. Statistical analysis was performed using an unpaired Student's t-test. * = P > 0.05, ** = P > 0.01, *** = P > 0.001.

Methods

Cells and reagents

Vero E6 and Calu-3 cells were obtained from the American Type Culture Collection (ATCC). Cells were maintained in Dulbecco's modified Eagle medium (DMEM) (Cellgro) supplemented with 25 mM HEPES (Cellgro) and 10% HyClone FetalClone II (GE) at 37° C and 5% CO_2. For virus infections, cells were grown in Eagle's Minimum Essential Medium (EMEM) (Cellgro) supplemented with 4% heat inactivated fetal bovine serum (FBS) (Gibco) at 37° C and 5% CO_2.

The SARS CoV 2 isolate USA-WA1/2020 was obtained from the Biological and Emerging Infections Resources Program (BEI Resources). Amlodipine, nifedipine, felodipine, verapamil, diltiazem and DTPA were purchased from Sigma Aldrich. 3-(4,5-dimethylthiazol-2-yl)-2,5-diphenyltetrazolium bromide (MMT) was obtained from Thermo Fisher. Crystal violet was purchased from VWR.

SARS-CoV-2 infections and TCID50 assays

Vero E6 and Calu-3 cells were grown to confluency under biosafety level-2 (BSL 2) conditions. Cells were then transferred to the BSL-3 lab, washed with DBPS and a volume of 200 µL infection media with SARS-

CoV-2 at an MOI of 0.1 was added to the cells. Cells were then incubated at 37° C and 5% CO_2 for 1 hour on a rocker. Cells were then supplemented with 800 µL infection media and appropriate concentrations of each drug were added. Amlodipine, nifedipine, felodipine and verapamil were dissolved in DMSO. Therefore, DMSO was used as a control at the same quantity that was applied for the highest drug concentration. After 24 hours the supernatants were harvested and stored at -80° C.

For the TCID50, Vero E6 cells were grown to confluency in 96 well plates and serial dilution of the samples were prepared. Undiluted and diluted samples were then added to the Vero E6 cells and grown for 72 hours at 37° C and 5% CO_2. After 72 hours supernatants were aspirated, and cells were fixed with 4% paraformaldehyde. Cells were then stained with 0.5% crystal violet and subsequently washed with dH_2O. Wells were scored and analyzed for living or dead cells according to the Reed-Muench method[30].

Cytotoxicity assay

The cytotoxicity of the calcium ion blocking drugs (amlodipine, nifedipine, felodipine, diltiazem) and calcium chelator (DTPA) on VeroE6 and Calu-3 cells were determined by an MTT Assay. A total of 5×10^5 VeroE6 cells/well, and 6.7×10^5 Calu-3 cells/well were incubated in the presence of the six calcium blocking drugs and calcium chelator at the concentrations of 10, 50, 100, and 500 µM for 24 hour at 37°C C and 5% CO_2 in a CO_2 incubator. After 24 hours incubation, cells were treated with MTT solution (5 mg/mL) and incubated for 4 hr at 37°C C and 5% CO_2 with rocking to allow purple formazan crystals to form. 50 µL DMSO was added into each well to dissolve the crystals. The absorbance was measured at 540 nm in a microplate reader (Bio-Tek Instrument Co., WA, USA).

References

1. Dong, E., Du, H. & Gardner, L. An interactive web-based dashboard to track COVID-19 in real time. *The Lancet Infectious Diseases* vol. 20 533–534 (2020).

2. Chan, J. F.-W. *et al.* Genomic characterization of the 2019 novel human-pathogenic coronavirus isolated from a patient with atypical pneumonia after visiting Wuhan. *Emerg. Microbes Infect.* **9**, 221–236 (2020).

3. Grein, J. *et al.* Compassionate Use of Remdesivir for Patients with Severe Covid-19. *N. Engl. J. Med.* **382**, 2327–2336 (2020).

4. Lai, A. L., Millet, J. K., Daniel, S., Freed, J. H. & Whittaker, G. R. The SARS-CoV Fusion Peptide Forms an Extended Bipartite Fusion Platform that Perturbs Membrane Order in a Calcium-Dependent Manner. *J. Mol. Biol.* **429**, 3875–3892 (2017).

5. Tang, T. *et al.* Coronavirus membrane fusion mechanism offers a potential target for antiviral development. (2020) doi:10.1016/j.antiviral.2020.104792.

6. Su, S. *et al.* Epidemiology, Genetic Recombination, and Pathogenesis of Coronaviruses. *Trends in Microbiology* vol. 24 490–502 (2016).

7. Zaki, A. M., Van Boheemen, S., Bestebroer, T. M., Osterhaus, A. D. M. E. & Fouchier, R. A. M. Isolation of a novel coronavirus from a man with pneumonia in Saudi Arabia. *N. Engl. J. Med.* **367**, 1814–1820 (2012).

8. World Health Organization. Middle East respiratory syndrome coronavirus (MERS-CoV). https://www.who.int/emergencies/mers-cov/en/ (2019).

9. WHO. *Consensus document on the epidemiology of severe acute respiratory syndrome (SARS)*. *Consensus document on the epidemiology of severe acute respiratory syndrome (SARS)* https://www.who.int/csr/sars/en/WHOconsensus.pdf (2003).

10. Drosten, C. *et al.* Identification of a Novel Coronavirus in Patients with Severe Acute Respiratory Syndrome. *N. Engl. J. Med.* **348**, 1967–1976 (2003).

11. World Health Organization. *Coronavirus Disease 2019 (COVID-19) Situation Reports - 72*. *WHO Situation report* https://www.who.int/emergencies/diseases/novel-coronavirus-2019/situation-reports (2020).

12. Wu, F. *et al.* A new coronavirus associated with human respiratory disease in China. *Nature* **579**, 265–269 (2020).

13. Boulware, D. R. *et al.* A Randomized Trial of Hydroxychloroquine as Postexposure Prophylaxis for Covid-19. *N. Engl. J. Med.* (2020) doi:10.1056/nejmoa2016638.

14. Hussain, M., Galvin, H. D., Haw, T. Y., Nutsford, A. N. & Husain, M. Drug resistance in influenza a virus: The epidemiology and management. *Infect. Drug Resist.* **10**, 121–134 (2017).

15. Straus, M. R. *et al.* Ca 2 Ions Promote Fusion of Middle East Respiratory Syndrome Coronavirus with Host Cells and Increase Infectivity VIRUS-CELL INTERACTIONS crossm Downloaded from.

jvi.asm.org 1 J. Virol. **94**, 426–446 (2020).

16. Matsuyama, S. *et al.* Efficient Activation of the Severe Acute Respiratory Syndrome Coronavirus Spike Protein by the Transmembrane Protease TMPRSS2. *J. Virol.* **84**, 12658–12664 (2010).

17. Kawase, M., Shirato, K., van der Hoek, L., Taguchi, F. & Matsuyama, S. Simultaneous Treatment of Human Bronchial Epithelial Cells with Serine and Cysteine Protease Inhibitors Prevents Severe Acute Respiratory Syndrome Coronavirus Entry. *J. Virol.* **86**, 6537–6545 (2012).

18. Fujioka, Y. *et al.* A Ca2+-dependent signalling circuit regulates influenza A virus internalization and infection. *Nat. Commun.* **4**, 1–13 (2013).

19. Nugent, K. M. & Shanley, J. D. Verapamil inhibits influenza A virus replication. *Arch. Virol.* **81**, 163–170 (1984).

20. Fujioka, Y. *et al.* A Sialylated Voltage-Dependent Ca 2+ Channel Binds Hemagglutinin and Mediates Influenza A Virus Entry into Mammalian Cells. *Cell Host Microbe* **23**, 809-818.e5 (2018).

21. Lavanya, M., Cuevas, C. D., Thomas, M., Cherry, S. & Ross, S. R. siRNA screen for genes that affect Junín virus entry uncovers voltage-gated calcium channels as a therapeutic target. *Sci. Transl. Med.* **5**, 204ra131-204ra131 (2013).

22. Wang, S. *et al.* Screening of FDA-Approved Drugs for Inhibitors of Japanese Encephalitis Virus Infection. *J. Virol.* **91**, (2017).

23. Wölfel, R. *et al.* Virological assessment of hospitalized patients with COVID-2019. *Nature* **581**, 465–469 (2020).

24. Löfdahl, C. -G & Barnes, P. J. Calcium, Calcium Channel Blockade and Airways Function. *Acta Pharmacol. Toxicol. (Copenh).* **58**, 91–111 (1986).

25. Du, W. *et al.* Excitation-contraction coupling in airway smooth muscle. *J. Biol. Chem.* **281**, 30143–30151 (2006).

26. Flores-Soto, E., Reyes-García, J., Sommer, B. & Montaño, L. M. Sarcoplasmic reticulum Ca2+ refilling is determined by L-type Ca2+ and store operated Ca2+ channels in guinea pig airway smooth muscle. *Eur. J. Pharmacol.* **721**, 21–28 (2013).

27. Chiu, K. Y., Li, J. G. & Lin, Y. Calcium channel blockers for lung function improvement in asthma: A

systematic review and meta-analysis. *Ann. Allergy, Asthma Immunol.* **119**, 518-523.e3 (2017).

28. Solaimanzadeh, I. Nifedipine and Amlodipine Are Associated With Improved Mortality and Decreased Risk for Intubation and Mechanical Ventilation in Elderly Patients Hospitalized for COVID-19. *Cureus* **12**, e8069–e8069 (2020).

29. Li, H. *et al.* Calcium channel blockers reduce severe fever with thrombocytopenia syndrome virus (SFTSV) related fatality. *Cell Res.* **29**, 739–753 (2019).

30. Lindenbach, B. D. Measuring HCV infectivity produced in cell culture and in vivo. *Methods Mol. Biol.* **510**, 329–336 (2009).

Acknowledgements

This projected was funded by Fast Grant, Mercatus Center. We would like to thank Paul Jeannette for his support for all the BSL-3 work and Dr. Hanno Andreas Ludewig for his critical input.

Author contributions

MRS: study design, experimental execution, data analysis, writing and editing of the manuscript. MB: experimental execution and data analysis. TT: experimental execution and data analysis. GRW: study design, writing and editing of the manuscript. SD: study design, writing and editing of the manuscript, funding acquisition.

Figures

Figure 1

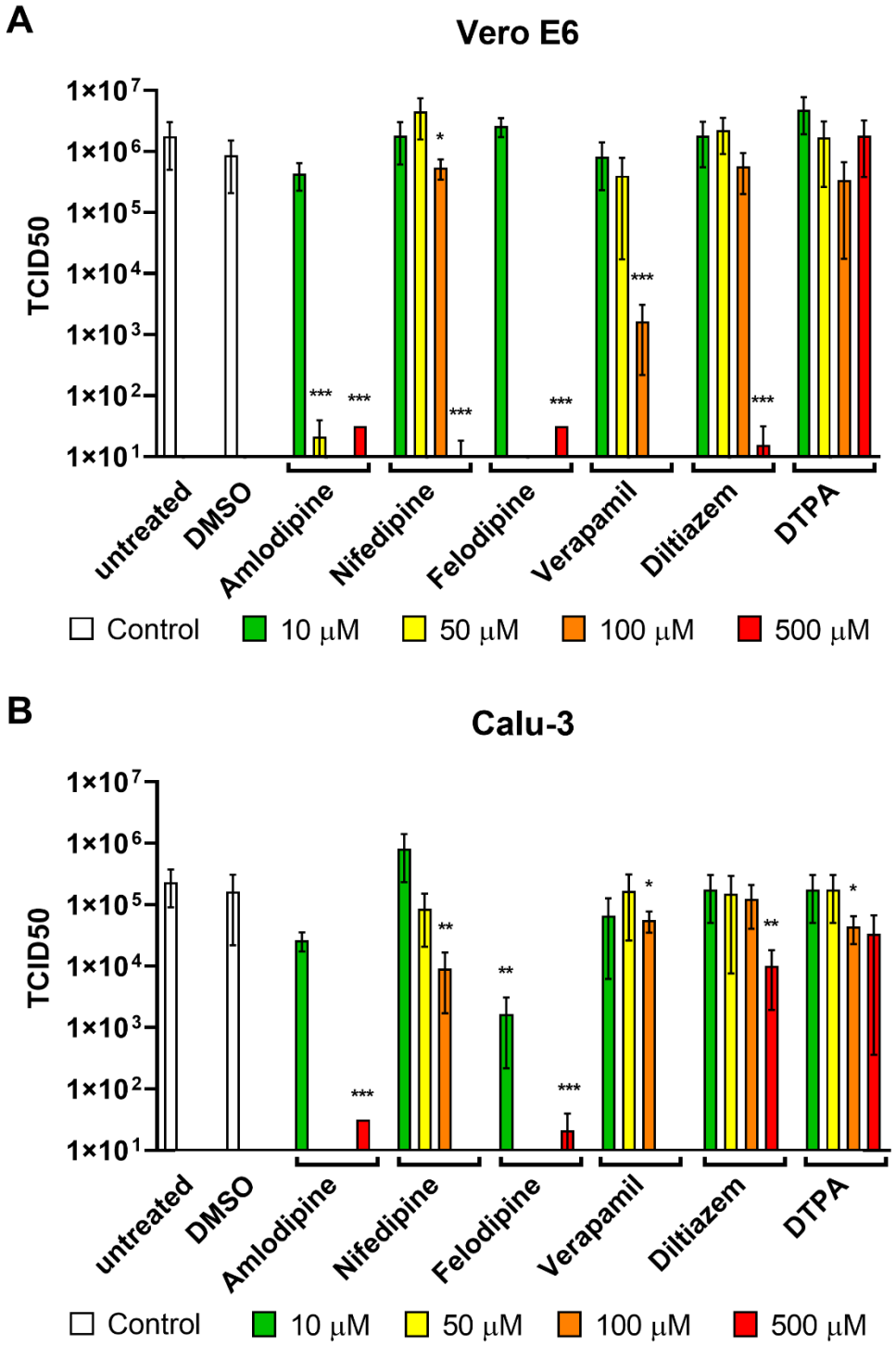

Figure 2

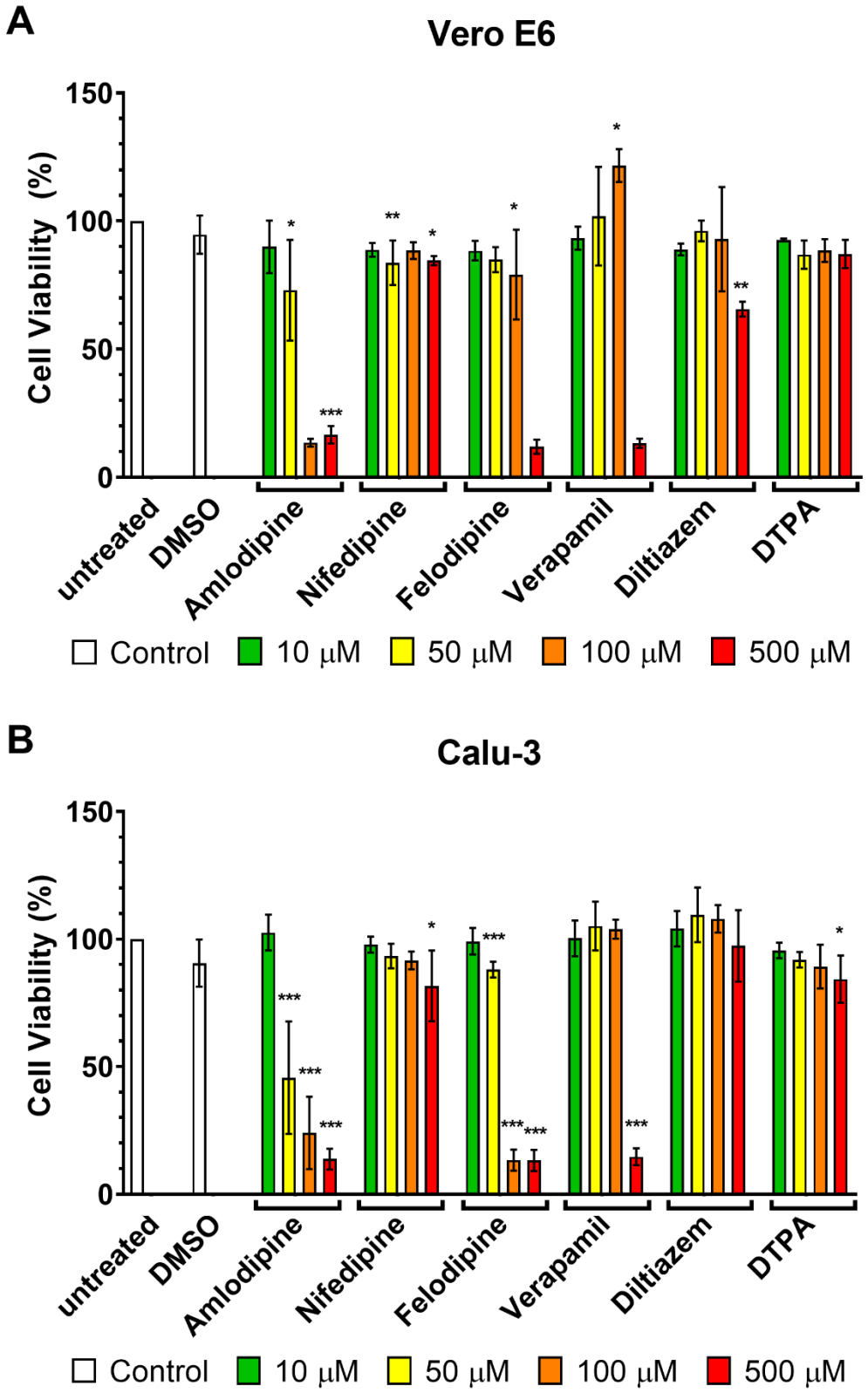
A
Vero E6
Cell Viability (%)
150
100
50
0
untreated
DMSO
Amlodipine
Nifedipine
Felodipine
Verapamil
Diltiazem
DTPA
Control
10 μM
50 μM
100 μM
500 μM
B
Calu-3
Cell Viability (%)
150
100
50
0
untreated
DMSO
Amlodipine
Nifedipine
Felodipine
Verapamil
Diltiazem
DTPA
Control
10 μM
50 μM
100 μM
500 μM